ESAIM: M2AN 43 (2009) 1099–1116
DOI: 10.1051/m2an/2009037

ESAIM: Mathematical Modelling and Numerical Analysis
www.esaim-m2an.org

IMPROVED SUCCESSIVE CONSTRAINT METHOD BASED *A POSTERIORI* ERROR ESTIMATE FOR REDUCED BASIS APPROXIMATION OF 2D MAXWELL'S PROBLEM

Yanlai Chen[1], Jan S. Hesthaven[1], Yvon Maday[1, 2] and Jerónimo Rodríguez[3]

Abstract. In *a posteriori* error analysis of reduced basis approximations to affinely parametrized partial differential equations, the construction of lower bounds for the coercivity and inf-sup stability constants is essential. In [Huynh *et al.*, *C. R. Acad. Sci. Paris Ser. I Math.* **345** (2007) 473–478], the authors presented an efficient method, compatible with an off-line/on-line strategy, where the on-line computation is reduced to minimizing a linear functional under a few linear constraints. These constraints depend on nested sets of parameters obtained iteratively using a greedy algorithm. We improve here this method so that it becomes more efficient and robust due to two related properties: (i) the lower bound is obtained by a monotonic process with respect to the size of the nested sets; (ii) less eigen-problems need to be solved. This improved evaluation of the inf-sup constant is then used to consider a reduced basis approximation of a parameter dependent electromagnetic cavity problem both for the greedy construction of the elements of the basis and the subsequent validation of the reduced basis approximation. The problem we consider has resonance features for some choices of the parameters that are well captured by the methodology.

Mathematics Subject Classification. 65N15, 65N30, 78A25.

Received August 28, 2008. Revised March 28, 2009.
Published online August 21, 2009.

1. Introduction

In the context of optimization, design or optimal control in many fields including, but not limited to, heat and mass transfer, solid mechanics, acoustics, fluid dynamics and electromagnetics, the numerical simulation of parametric problems written under the weak form: find $u(\nu)$ in an Hilbert space X such that

$$a(u(\nu), v; \nu) = f(v; \nu), \quad \forall v \in X, \tag{1.1}$$

has to be done for many input parameter ν – a P-tuple with moderate P – chosen in a given parameter set $\mathcal{D}$

Keywords and phrases. Reduced basis method, successive constraint method, inf-sup constant, *a posteriori* error estimate, Maxwell's equation, discontinuous Galerkin method.

[1] Division of Applied Mathematics, Brown University, 182 George St, Providence, RI 02912, USA. Yanlai_Chen@brown.edu; Jan.Hesthaven@Brown.edu
[2] Université Pierre et Marie Curie-Paris 6, UMR 7598, Laboratoire J.-L. Lions, 75005 Paris, France. maday@ann.jussieu.fr
[3] Departamento de Matemática Aplicada, Universidade de Santiago de Compostela, 15782 Santiago de Compostela, Spain. jeronimo.rodriguez@usc.es

Article published by EDP Sciences

(a closed and bounded subset of $\mathbb{R}^P$). In the previous problem a and f are bilinear and linear forms, respectively, associated to the PDE. The natural hypotheses over $a(w, v; \nu)$ that make problem (1.1) well-posed are

– uniform continuity, that is, there exists a uniformly bounded $\gamma(\nu)$ such that

$$|a(w, v; \nu)| \ \leq \ \gamma(\nu)\|w\|_X\|v\|_X, \quad \forall w,\ v \in X,\ \forall \nu \in \mathcal{D};$$

– uniform inf-sup condition

$$0 < \beta_0 < \beta(\nu) \equiv \inf_{\omega \in X} \sup_{v \in X} \frac{|a(\omega, v; \nu)|}{\|\omega\|_X\|v\|_X} = \inf_{\omega \in X} \frac{\|a(\omega, \cdot; \nu)\|_{X'}}{\|\omega\|_X}, \ \forall \nu \in \mathcal{D}.$$

It follows directly from these assumptions that (1.1) admits a unique solution. A finite element (FE) discretization of problem (1.1) is a standard way to approximate its solution $u^{\mathcal{N}}(\nu) \simeq u(\nu)$: Given $\nu \in \mathcal{D} \subset \mathbb{R}^P$, find $u^{\mathcal{N}}(\nu) \in X^{\mathcal{N}}$ satisfying

$$a^{\mathcal{N}}(u^{\mathcal{N}}(\nu), v; \nu) = f^{\mathcal{N}}(v; \nu)^4, \quad \forall v \in X^{\mathcal{N}}.$$

Here $X^{\mathcal{N}}$ is the finite element space approximating X with $\dim(X^{\mathcal{N}}) \equiv \mathcal{N}$. We assume $u^{\mathcal{N}}$ provides a *reference* solution (called truth approximation throughout the paper) that is accurate enough for all $\nu \in \mathcal{D}$. The well-posedness is a consequence of the discrete inf-sup condition,

$$0 < \beta_0^{\mathcal{N}} < \beta^{\mathcal{N}}(\nu) \equiv \inf_{\omega \in X^{\mathcal{N}}} \sup_{v \in X^{\mathcal{N}}} \frac{|a^{\mathcal{N}}(\omega, v; \nu)|}{\|\omega\|_{X^{\mathcal{N}}}\|v\|_{X^{\mathcal{N}}}}, \ \forall \nu \in \mathcal{D}.$$

It is most of the times infeasible to directly solve the finite element problem too many times because of the high marginal cost resulting from the large dimension of the discrete systems to be solved (equal to the dimension $\mathcal{N}$ of the finite element space).

The reduced basis method (RBM) [2,6,12,14,15,17] has emerged as a very efficient and accurate method in this scenario. The fundamental observation that is recognized and exploited by the RBM is the following. Instead of being an arbitrary element of $X^{\mathcal{N}}$, $u^{\mathcal{N}}(\nu)$ typically resides on $\mathcal{M}^\nu = \{u^{\mathcal{N}}(\nu),\ \nu \in \mathcal{D}\}$ that can be well approximated by a finite-dimensional space whenever the set $\mathcal{M}^\nu$ has a small Kolmogorov width in X. The idea is then to propose an approximation of $\mathcal{M}^\nu$ by

$$W^N = \text{span}\{u^{\mathcal{N}}(\nu_1), \ldots, u^{\mathcal{N}}(\nu_N)\}$$

where, $u^{\mathcal{N}}(\nu_1), \ldots, u^{\mathcal{N}}(\nu_N)$ are N ($\ll \mathcal{N}$) truth approximations corresponding to the parameters $\{\nu_1, \ldots, \nu_N\}$ selected according to a judicious sampling strategy [10]. For a given ν, we now seek the Galerkin projection onto this N-dimensional approximation space W^N, as the solution $u^N(\nu)$. The on-line computation is $\mathcal{N}$-independent, thanks to the assumption that the (bi)linear forms are affine[5] and the fact that they can be approximated by affine (bi)linear forms when they are nonaffine [1,5]. Hence, the on-line part is very efficient.

In order to be able to "optimally" find the N parameters and to assure the fidelity of the reduced basis solution $u^N(\nu)$ to approximate the truth solution $u^{\mathcal{N}}(\nu)$, we need the inf-sup number, $\beta^{\mathcal{N}}(\nu)$, of the bilinear form [9,11,16–18]: indeed, one can prove that when $a^{\mathcal{N}}$ is symmetric, we have the following upper and lower bounds for the error of the reduced basis solution, $\|u^{\mathcal{N}}(\nu) - u^N(\nu)\|_{X^{\mathcal{N}}}$,

$$\|r(\cdot, \nu)\|_{(X^{\mathcal{N}})'}/\gamma(\nu) \ \leq \ \|u^{\mathcal{N}}(\nu) - u^N(\nu)\|_{X^{\mathcal{N}}} \ \leq \ \|r(\cdot, \nu)\|_{(X^{\mathcal{N}})'}/\beta^{\mathcal{N}}(\nu). \tag{1.2}$$

Here, the residual is defined as $r(v, \nu) = f(v; \nu) - a^{\mathcal{N}}(u^N(\nu), v; \nu)$, and $\|\cdot\|_{(X^{\mathcal{N}})'}$ is the dual norm.

[4] A notation consistent with the reduced basis context is used here. It corresponds to u_h, a_h and f_h in the finite element context, where a_h and f_h are finite dimensional approximations of $a(\cdot, \cdot; \cdot)$ and $f(\cdot; \cdot)$ respectively and u_h is the solution of the discrete problem.

[5] $a(w, v; \nu) \equiv \sum_{q=1}^{Q_a} \Theta_a^q(\nu)\, a^q(w, v), \quad \forall w, v \in X^{\mathcal{N}}$, $f(v; \nu) \equiv \sum_{q=1}^{Q_f} \Theta_f^q(\nu)\, f^q(v), \quad \forall v \in X^{\mathcal{N}}$.

It is therefore crucial to find a lower bound $\beta_{LB}(\nu)$ of $\beta^{\mathcal{N}}(\nu)$ since the latter is generally not known. The construction of $\beta_{LB}(\nu)$ is a "bottleneck" of RBM, especially in the non-coercive case. Different ideas have come up in the literature for the coercive and non-coercive cases, see [11,13] and the references therein. Recently, Huynh *et al.* [8] have proposed an attractive strategy for this purpose – the successive constraint method (SCM) – based on linear programming techniques that is more efficient than the earlier ones.

In this paper, we study, improve and test the SCM on non-coercive problems exemplified by an electromagnetic cavity problem. The *new* SCM is superior to the previous [8] in the following two ways:

- first, the method is more stable in the sense that β_{LB} is obtained by a monotonic process (in contrast to being oscillatory before);
- second, we need to solve less eigen-problems.

This result was briefly announced in a short note [4].

The remaining part of the paper is organized as follows. In Section 2, we describe the original and the improved SCM and prove the above-mentioned properties. We then show numerical results in Section 3 to verify our claims. Some concluding remarks are provided in Section 4.

2. Successive constraint method

In this section, we first state the SCM proposed in [8] for completeness. Then, we describe the improvements.

2.1. The original method

We describe the SCM for the coercive and then the non-coercive case.

2.1.1. *Coercive case*

Given an affine bilinear form

$$a^{\mathcal{N}}(w,v;\nu) \equiv \sum_{q=1}^{Q} \Theta^q(\nu)\, a_q^{\mathcal{N}}(w,v), \quad \forall w,\, v \in X^{\mathcal{N}},$$

the coercivity constant is

$$\alpha^{\mathcal{N}}(\nu) \equiv \inf_{w\in X^{\mathcal{N}}} \frac{a^{\mathcal{N}}(w,w;\nu)}{\|w\|^2_{X^{\mathcal{N}}}} = \inf_{w\in X^{\mathcal{N}}} \sum_{q=1}^{Q} \Theta^q(\nu) \frac{a_q^{\mathcal{N}}(w,w)}{\|w\|^2_{X^{\mathcal{N}}}} = \inf_{w\in X^{\mathcal{N}}} \sum_{q=1}^{Q} \Theta^q(\nu) y_q(w).$$

Here, we set $y_q(w) = \frac{a_q^{\mathcal{N}}(w,w)}{\|w\|^2_{X^{\mathcal{N}}}}$. Obviously, $(y_1(w), \ldots, y_Q(w))$ belongs to the following set

$$\mathcal{Y} \equiv \left\{ y = (y_1, \ldots, y_Q) \in \mathbb{R}^Q \mid \exists\, w \in X^{\mathcal{N}} \text{ s.t. } y_q = y_q(w),\ 1 \le q \le Q \right\}.$$

Having defined the set $\mathcal{Y}$, our coercivity constant can be found by solving the following minimization problem:

$$\alpha^{\mathcal{N}}(\nu) = \inf_{y\ \in \mathcal{Y}} \mathcal{J}(\nu; y), \tag{2.1}$$

where the objective function $\mathcal{J} : \mathcal{D} \times \mathbb{R}^Q \to \mathbb{R}$ is defined as

$$\mathcal{J}(\nu; y) = \sum_{q=1}^{Q} \Theta^q(\nu) y_q.$$

Problem (2.1) appears like a minimization problem of a linear functional over a compact subset of $\mathbb{R}^Q$.

We only need to characterize the set $\mathcal{Y}$ now. The idea of SCM is to build two sets $\mathcal{Y}_{LB}$ and $\mathcal{Y}_{UB}$ over which the minimization of $\mathcal{J}$ is feasible and satisfy $\mathcal{Y}_{UB} \subset \mathcal{Y} \subset \mathcal{Y}_{LB}$. Therefore, we can perform the minimization on these two sets to obtain an upper bound and a lower bound for $\alpha^{\mathcal{N}}(\nu)$. For this purpose, we define

$$\sigma_q^- \equiv \inf_{w \in X^{\mathcal{N}}} y_q(w), \quad \sigma_q^+ \equiv \sup_{w \in X^{\mathcal{N}}} y_q(w), \quad 1 \le q \le Q,$$

and let $\mathcal{B}_Q \equiv \Pi_{q=1}^Q [\sigma_q^-, \sigma_q^+] \subset \mathbb{R}^Q$. Obviously, $\mathcal{Y} \subset \mathcal{B}_Q$.

To properly define $\mathcal{Y}_{LB}$ and $\mathcal{Y}_{UB}$, we also need to introduce two parameter sets $\Xi \equiv \{\nu_1 \in \mathcal{D}, \ldots, \nu_J \in \mathcal{D}\}$ and $C_K \equiv \{\nu_1 \in \mathcal{D}, \ldots, \nu_K \in \mathcal{D}\}$. Ξ is a (rather large) sample set of grid points in the parameter domain (*e.g.* defined from a mesh) and C_K is any subset of Ξ. Let $P_M(\nu; E)$ denote the M points closest to ν in E with E being Ξ or C_K.

We are now ready to define $\mathcal{Y}_{LB}$ and $\mathcal{Y}_{UB}$: For given C_K (and $M_\alpha \in \mathbb{N}$, $M_+ \in \mathbb{N}$, and Ξ), we define

$$\mathcal{Y}_{LB}(\nu; C_K) \equiv \left\{ y \in \mathcal{B}_Q \mid \sum_{q=1}^Q \Theta^q(\nu') y_q \ge \alpha^{\mathcal{N}}(\nu'),\ \forall \nu' \in P_{M_\alpha}(\nu; C_K); \right. \\ \left. \sum_{q=1}^Q \Theta^q(\nu') y_q \ge 0,\ \forall \nu' \in P_{M_+}(\nu; \Xi) \right\}, \tag{2.2}$$

and $\mathcal{Y}_{UB}(C_K) \equiv \{y^*(\nu_k),\ 1 \le k \le K\}$ for $y^*(\nu) \equiv \operatorname{argmin}_{y \in \mathcal{Y}} \mathcal{J}(\nu; y)$. We then define

$$\alpha_{LB}(\nu; C_K) = \inf_{y \in \mathcal{Y}_{LB}(\nu; C_K)} \mathcal{J}(\nu; y), \tag{2.3}$$

and

$$\alpha_{UB}(\nu; C_K) = \inf_{y \in \mathcal{Y}_{UB}(C_K)} \mathcal{J}(\nu; y), \tag{2.4}$$

to obtain:

Proposition 2.1. *For given C_K (and $M_\alpha \in \mathbb{N}$, $M_+ \in \mathbb{N}$, and Ξ), $\alpha_{LB}(\nu; C_K) \le \alpha^{\mathcal{N}}(\nu) \le \alpha_{UB}(\nu; C_K)$, $\forall \nu \in \mathcal{D}$.*

Proof. It is simple to recognize that $\mathcal{Y}_{UB} \subset \mathcal{Y} \subset \mathcal{Y}_{LB}$. The result then follows. □

Note that (2.2), (2.3) is in fact a Linear Program (LP); our LP (2.3) contains Q design variables and $2Q + M_\alpha + M_+$ (one-sided) inequality constraints: the operation count for the on-line stage $\nu \to \alpha_{LB}(\nu)$ is independent of $\mathcal{N}$.

It only remains to determine C_K. It is constructed by an off-line "greedy" algorithm. Given $M_\alpha \in \mathbb{N}$, $M_+ \in \mathbb{N}$, Ξ, and a tolerance $\epsilon_\alpha \in [0, 1]$, the algorithm reads:

(1) Set $K = 1$ and choose $C_1 = \{\nu_1\}$ arbitrarily.
(2) Find $\nu_{K+1} = \operatorname{argmax}_{\nu \in \Xi} \frac{\alpha_{UB}(\nu; C_K) - \alpha_{LB}(\nu; C_K)}{\alpha_{UB}(\nu; C_K)}$.
(3) Update $C_{K+1} = C_K \cup \nu_{K+1}$.
(4) Repeat (2) and (3) until $\max_{\nu \in \Xi} \frac{\alpha_{UB}(\nu; C_{K_{max}}) - \alpha_{LB}(\nu; C_{K_{max}})}{\alpha_{UB}(\nu; C_{K_{max}})} \le \epsilon_\alpha$.

We note that the off-line computations are:

(1) $2Q + K_{\max}$ eigen-problems to form $\mathcal{B}_Q$ and to obtain $y^*(\nu_k)$, $\alpha^{\mathcal{N}}(\nu_k)$.
(2) $O(\mathcal{N} Q K_{\max})$ operations to form $\mathcal{Y}_{UB}$.
(3) $J K_{\max}$ LPs of size $O(Q + M_\alpha + M_+)$.

2.1.2. *Non-coercive case*

For the non-coercive case, we need to find a lower bound of the inf-sup number,

$$\beta^{\mathcal{N}}(\nu) \equiv \inf_{\omega \in X^{\mathcal{N}}} \sup_{v \in X^{\mathcal{N}}} \frac{|a^{\mathcal{N}}(\omega, v; \nu)|}{\|\omega\|_{X^{\mathcal{N}}} \|v\|_{X^{\mathcal{N}}}}.$$

If we define an operator $T^{\nu} : X^{\mathcal{N}} \to X^{\mathcal{N}}$ as $(T^{\nu} w, v)_{X^{\mathcal{N}}} = a^{\mathcal{N}}(w, v; \nu),\ \forall v \in X^{\mathcal{N}}$, it is easy to show that

$$\beta^{\mathcal{N}}(\nu) = \inf_{w \in X^{\mathcal{N}}} \frac{\|T^{\nu} w\|_{X^{\mathcal{N}}}}{\|w\|_{X^{\mathcal{N}}}},$$

which means

$$(\beta^{\mathcal{N}}(\nu))^2 = \inf_{w \in X^{\mathcal{N}}} \frac{(T^{\nu} w, T^{\nu} w)_{X^{\mathcal{N}}}}{\|w\|^2_{X^{\mathcal{N}}}}.$$

To expand it, we need to define operators $T^q : X^{\mathcal{N}} \to X^{\mathcal{N}}$ as

$$(T^q w, v)_{X^{\mathcal{N}}} = a^{\mathcal{N}}_q(w, v),\ \forall v \in X^{\mathcal{N}},\ 1 \le q \le Q.$$

Realizing $T^{\nu} w \equiv \sum_{q=1}^{Q} \Theta^q(\nu) T^q w$, we can expand $(\beta^{\mathcal{N}}(\nu))^2$ as

$$(\beta^{\mathcal{N}}(\nu))^2 = \inf_{w \in X^{\mathcal{N}}} \sum_{q'=1}^{Q} \sum_{q''=q'}^{Q} (2 - \delta_{q' q''}) \Theta^{q'}(\nu) \Theta^{q''}(\nu) \frac{(T^{q'} w, T^{q''} w)_{X^{\mathcal{N}}}}{\|w\|^2_{X^{\mathcal{N}}}}.$$

Here, $\delta_{q' q''}$ is the Kronecker delta. Next, we identify

$$(2 - \delta_{q' q''}) \Theta^{q'}(\nu) \Theta^{q''}(\nu),\ 1 \le q' \le q'' \le Q \longmapsto \hat{\Theta}^q(\nu),\ 1 \le q \le \hat{Q} \equiv \frac{Q(Q+1)}{2},$$

$$(T^{q'} w, T^{q''} w)_{X^{\mathcal{N}}},\ 1 \le q' \le q'' \le Q \longmapsto \hat{a}^{\mathcal{N}}_q(w, v),\ 1 \le q \le \hat{Q},$$

and obtain

$$(\beta^{\mathcal{N}}(\nu))^2 \equiv \inf_{w \in X^{\mathcal{N}}} \sum_{q=1}^{\hat{Q}} \hat{\Theta}^q(\nu) \frac{\hat{a}^{\mathcal{N}}_q(w, w)}{\|w\|^2_{X^{\mathcal{N}}}}. \tag{2.5}$$

Hence $(\beta^{\mathcal{N}}(\nu))^2$ can be interpreted as the coercivity constant for the bilinear form

$$\hat{\alpha}^{\mathcal{N}}(\nu) \equiv \inf_{w \in X^{\mathcal{N}}} \sum_{q=1}^{\hat{Q}} \hat{\Theta}^q(\nu) \frac{\hat{a}^{\mathcal{N}}_q(w, w)}{\|w\|^2_{X^{\mathcal{N}}}}.$$

And we may then directly apply the SCM procedure defined above to (2.5).

2.2. **Some improvements**

2.2.1. *On the definition of* $\mathcal{Y}_{LB}(\nu; C_K)$

We note that in (2.2), zero is used in the constraints for the M_+ members of $P_{M_+}(\nu; \Xi)$. However, we have a lower bound that we can evaluate on the set C_{K-1} available. These quantities are certainly better candidates

to be used as the constraints. This motivates replacement of (2.2) by

$$\mathcal{Y}_{LB}(\nu; C_K) \equiv \Bigg\{ y \in \mathcal{B}_Q \mid \sum_{q=1}^{Q} \Theta^q(\nu') y_q \geq \alpha^{\mathcal{N}}(\nu'),\ \forall \nu' \in P_{M_\alpha}(\nu; C_K); \\ \sum_{q=1}^{Q} \Theta^q(\nu') y_q \geq \alpha_{LB}(\nu', C_{K-1}),\ \forall \nu' \in P_{M_+}(\nu; \Xi \backslash C_K) \Bigg\}. \tag{2.6}$$

Note that we define trivially, $\alpha_{LB}(\nu, C_0) \equiv 0,\ \forall \nu \in \Xi$. Then, we obtain

Proposition 2.2. *With $\mathcal{Y}_{LB}(\nu; C_K)$ defined as above and the greedy algorithm as in the previous subsection, we have for any $\nu \in \Xi$, as K increases,*

(1) *$\alpha_{LB}(\nu, C_K)$ is nondecreasing.*
(2) *$\alpha_{UB}(\nu, C_K)$ is nonincreasing.*
(3) *$\frac{\alpha_{UB}(\nu, C_K) - \alpha_{LB}(\nu, C_K)}{\alpha_{UB}(\nu, C_K)}$ is nonincreasing.*

Proof. (1) Simply follows from the fact that for any $\nu \in \Xi$, $\sum_{q=1}^{Q} \Theta^q(\nu) y_q \geq \alpha_{LB}(\nu, C_{K-1})$ is included as one constraint when we are looking for $\alpha_{LB}(\nu, C_K)$. This means the *updated* lower bound is getting no smaller. (2) is a direct consequence of the definition of $\alpha_{UB}(\nu, C_K)$, and (3) follows from (1) and (2). □

Remark 2.1. The *new* SCM is more efficient than the original formulation, both off-line and on-line, in the following two ways:

(1) The new method is likely to solve less eigen-problems than the old SCM to obtain the lower bound of the same quality. This is because, on the same set C_K, the new method provides larger lower bound. The final set C_K that meets the stopping criteria is going to be no larger than that for the original method.
(2) With the same settings, the LP in the new method shall take less time to solve since the constraints are stricter.

Remark 2.2. In the greedy algorithm, when we are searching for ν_{K+1}, we need $\alpha_{LB}(\nu, C_K)$ for any $\nu \in \Xi$. We note that it is not needed to solve the LP for every ν. In fact, $\alpha_{LB}(\nu, C_K) = \alpha_{LB}(\nu, C_{K-1})$ when $P_{M_\alpha}(\nu; C_K) = P_{M_\alpha}(\nu; C_{K-1})$ and $P_{M_+}(\nu; \Xi \backslash C_K) = P_{M_+}(\nu; \Xi \backslash C_{K-1})$. This means that we only solve LP for the ν's that have $P_{M_\alpha}(\nu; C_K) \neq P_{M_\alpha}(\nu; C_{K-1})$ or $P_{M_+}(\nu; \Xi \backslash C_K) \neq P_{M_+}(\nu; \Xi \backslash C_{K-1})$, *i.e.*, only when $\nu_K \in P_{M_\alpha}(\nu; C_K)$ or $\nu_K \in P_{M_+}(\nu; \Xi \backslash C_{K-1})$. This substantially reduces the runtime for solving the LPs and thus the dominant computations are for the eigenvalue-problems.

Remark 2.3. When searching for ν_{K+1} in the greedy algorithm, we need to go through the set Ξ. It is preferred to do this hierarchically by exploring a uniform mesh of $[0, 1]$ with 2^p elements in which we visit the grid points in the following order: $0, 1; \frac{1}{2}; \frac{1}{4}, \frac{3}{4}; \frac{1}{8}, \frac{3}{8}, \frac{5}{8}, \frac{7}{8}$... The extension to multidimensional problems is straightforward.

2.2.2. *On the conversion of the non-coercive case*

For the non-coercive case, we can expand

$$(\beta^{\mathcal{N}}(\nu))^2 = \inf_{w \in X^{\mathcal{N}}} \frac{(T^\nu w, T^\nu w)_{X^{\mathcal{N}}}}{\|w\|^2_{X^{\mathcal{N}}}}$$

as

$$
\begin{aligned}
(\beta^{\mathcal{N}}(\nu))^2 &= \inf_{w\in X^{\mathcal{N}}} \sum_{q'=1}^{Q}\sum_{q''=1}^{Q} Z_{q''}^{q'}(\nu)\frac{(T^{q'}w, T^{q''}w)_{X^{\mathcal{N}}}}{\|w\|_{X^{\mathcal{N}}}^2} \\
&= \inf_{w\in X^{\mathcal{N}}} \sum_{q=1}^{Q} Z_q^q(\nu)\frac{(T^q w, T^q w)_{X^{\mathcal{N}}}}{\|w\|_{X^{\mathcal{N}}}^2} + \sum_{q'=1}^{Q}\sum_{q''=q'+1}^{Q} Z_{q''}^{q'}(\nu)\frac{(T^{q'}w, T^{q''}w)_{X^{\mathcal{N}}} + (T^{q''}w, T^{q'}w)_{X^{\mathcal{N}}}}{\|w\|_{X^{\mathcal{N}}}^2} \\
&= \inf_{w\in X^{\mathcal{N}}} \sum_{q=1}^{Q}\left(Z_q^q(\nu) - \sum_{q'=1,q'\neq q}^{Q} Z_q^{q'}(\nu)\right)\frac{(T^q w, T^q w)_{X^{\mathcal{N}}}}{\|w\|_{X^{\mathcal{N}}}^2} \\
&\quad + \sum_{q'=1}^{Q}\sum_{q''=q'+1}^{Q} Z_{q''}^{q'}(\nu)\frac{(T^{q'}w + T^{q''}w, T^{q'}w + T^{q''}w)_{X^{\mathcal{N}}}}{\|w\|_{X^{\mathcal{N}}}^2},
\end{aligned} \tag{2.7}
$$

with $Z_{q''}^{q'}(\nu) = \Theta^{q'}(\nu)\Theta^{q''}(\nu)$.

This leads to symmetric and positive semi-definite parameter independent bilinear forms, whereas the bilinear forms in the previous expansion are nonsymmetric and could be negative definite.

Before extending this to the complex case, we interpret the expansion above in terms of matrices: if we let $\boldsymbol{w}$ denote the vector of degrees of freedom for $w \in X^{\mathcal{N}}$ and $M_{T^{q'},T^{q''}}$ denote the matrix corresponding to $(T^{q'}w, T^{q''}w)_{X^{\mathcal{N}}}$, we rewrite (2.7) as

$$
\begin{aligned}
(\beta^{\mathcal{N}}(\nu))^2 &= \inf_{w\in X^{\mathcal{N}}} \sum_{q'=1}^{Q}\sum_{q''=1}^{Q} Z_{q''}^{q'}(\nu)\frac{\boldsymbol{w}^T M_{T^{q'},T^{q''}}\boldsymbol{w}}{\|w\|_{X^{\mathcal{N}}}^2} \\
&= \inf_{w\in X^{\mathcal{N}}} \sum_{q=1}^{Q}\left(Z_q^q(\nu) - \sum_{q'=1,q'\neq q}^{Q} Z_q^{q'}(\nu)\right)\frac{\boldsymbol{w}^T M_{T^q,T^q}\boldsymbol{w}}{\|w\|_{X^{\mathcal{N}}}^2} \\
&\quad + \sum_{q'=1}^{Q}\sum_{q''=q'+1}^{Q} Z_{q''}^{q'}(\nu)\frac{\boldsymbol{w}^T M_{T^{q'}+T^{q''},T^{q'}+T^{q''}}\boldsymbol{w}}{\|w\|_{X^{\mathcal{N}}}^2}.
\end{aligned}
$$

When $\Theta^q(\nu)$ is complex, we have

$$
\begin{aligned}
(\beta^{\mathcal{N}}(\nu))^2 &= \inf_{w\in X^{\mathcal{N}}} \sum_{q'=1}^{Q}\sum_{q''=1}^{Q} Z_{q''}^{q'}(\nu)\frac{\boldsymbol{w}^H M_{T^{q'},T^{q''}}\boldsymbol{w}}{\|w\|_{X^{\mathcal{N}}}^2} \\
&= \inf_{w\in X^{\mathcal{N}}} \sum_{q=1}^{Q} Z_q^q(\nu)\frac{\boldsymbol{w}^H M_{T^q,T^q}\boldsymbol{w}}{\|w\|_{X^{\mathcal{N}}}^2} + \sum_{q'=1}^{Q}\sum_{q''=q'+1}^{Q}\frac{Z_{q''}^{q'}(\nu)\boldsymbol{w}^H M_{T^{q'},T^{q''}}\boldsymbol{w} + Z_{q'}^{q''}(\nu)\boldsymbol{w}^H M_{T^{q''},T^{q'}}\boldsymbol{w}}{\|w\|_{X^{\mathcal{N}}}^2} \\
&= \inf_{w\in X^{\mathcal{N}}} \sum_{q=1}^{Q} Z_q^q(\nu)\frac{\boldsymbol{w}^H M_{T^q,T^q}\boldsymbol{w}}{\|w\|_{X^{\mathcal{N}}}^2} + \sum_{q'=1}^{Q}\sum_{q''=q'+1}^{Q}\frac{\boldsymbol{w}^H\left(Z_{q''}^{q'}(\nu)M_{T^{q'},T^{q''}} + Z_{q'}^{q''}(\nu)M_{T^{q'},T^{q''}}{}^T\right)\boldsymbol{w}}{\|w\|_{X^{\mathcal{N}}}^2}.
\end{aligned}
$$

Here, $Z_{q''}^{q'}(\nu) = \Theta^{q'}(\nu)\bar{\Theta}^{q''}(\nu) = \bar{Z}_{q'}^{q''}(\nu)$.

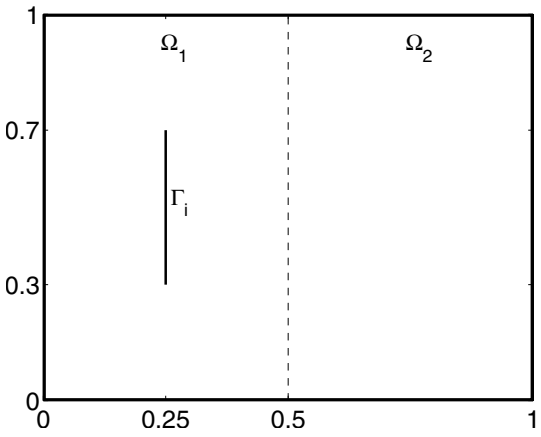

FIGURE 1. The electromagnetic cavity problem.

Note that, when z is a complex number, X is a complex vector and A is a real matrix, we have that

$$\begin{aligned} X^H\left(z\,A+\bar{z}\,A^T\right)X &= 2\Re z\left(\Re X^T\Im X^T\right)\begin{pmatrix} A & 0\\ 0 & A\end{pmatrix}\begin{pmatrix}\Re X\\ \Im X\end{pmatrix}+2\Im z\left(\Re X^T\Im X^T\right)\begin{pmatrix} 0 & -A\\ A & 0\end{pmatrix}\begin{pmatrix}\Re X\\ \Im X\end{pmatrix}\\ &= 2\Re z\left(\Re X^T\Im X^T\right)\begin{pmatrix} \frac{A+A^T}{2} & 0\\ 0 & \frac{A+A^T}{2}\end{pmatrix}\begin{pmatrix}\Re X\\ \Im X\end{pmatrix}\\ &\quad+2\Im z\left(\Re X^T\Im X^T\right)\begin{pmatrix} 0 & \frac{A^T-A}{2}\\ \frac{A-A^T}{2} & 0\end{pmatrix}\begin{pmatrix}\Re X\\ \Im X\end{pmatrix}. \end{aligned}$$

Here, $\Re$ and $\Im$ indicate real and imaginary parts, respectively. We can then proceed as in the real case by replacing $M_{T^{q'},T^{q''}}+M_{T^{q''},T^{q'}}$ by $M_{T^{q'}+T^{q''},T^{q'}+T^{q''}}-M_{T^{q'},T^{q'}}-M_{T^{q''},T^{q''}}$.

3. NUMERICAL RESULTS

It is relatively easy to find the coercivity constant for the coercive problems. The available methods, see [11,13] and the references therein, are more challenging when it comes to non-coercive problems. There is an urgent need for efficient methods especially when the inf-sup number may go to zero, as it is the case, for example, around resonances in electromagnetics. The motivation for the preceding analysis comes from the problem we want to approximate with reduced basis method that is a challenging electromagnetic cavity problem where resonances do occur.

3.1. **Problem setup**

We are looking for the frequency-domain solution of the two-dimensional Maxwell's equations in normalized differential form in Ω,

$$\begin{cases} -\epsilon\omega^2 E_x+\frac{1}{\mu}\frac{\partial}{\partial y}\left(\frac{\partial E_y}{\partial x}-\frac{\partial E_x}{\partial y}\right)=\mathrm{i}\omega J_x\\ -\epsilon\omega^2 E_y-\frac{1}{\mu}\frac{\partial}{\partial x}\left(\frac{\partial E_y}{\partial x}-\frac{\partial E_x}{\partial y}\right)=\mathrm{i}\omega J_y\end{cases} \tag{3.1}$$

with boundary condition $E_x\,\hat{n}_y-E_y\,\hat{n}_x=0$ on $\partial\Omega$, $(\hat{n}_x,\hat{n}_y)$ being the unit outward normal of $\partial\Omega$, $X=H(\mathrm{curl})$.

Here, see Figure 1, $\Omega=\Omega_1\bigcup\Omega_2$ with $\Omega_1=[0,0.5]\times[0,1]$, $\Omega_2=[0.5,1]\times[0,1]$, $\epsilon|_{\Omega_i}=\epsilon_i$, $\mu|_{\Omega_i}=\mu_i$ for $i=1,2$ with the range of ϵ_i, μ_i to be specified later. We set $J_x=0$, $J_y=\cos(\omega(y-\frac{1}{2}))\delta_{\Gamma_i}$ with $\Gamma_i=0.25\times[0.3,0.7]$.

Given a triangulation (locally refined around the tips of Γ_i) of Ω, $\Omega^{\mathcal{N}} = \bigcup_{d=1}^{D} T_d$, we set $X^{\mathcal{N}} = \{v \in L^2(\Omega^{\mathcal{N}}) \,|\, v \in \oplus_{d=1}^{D} P^4(T_d)\}$.

We identify $\frac{1}{i\omega}\left(\frac{\partial E_x}{\partial y} - \frac{\partial E_y}{\partial x}\right)$ as H_z and apply the discontinuous Galerkin method, see [7], and the weak formulation is: find $(E_x, E_y, H_z) \in (X^{\mathcal{N}})^3$ such that

$$\begin{cases} \mathrm{i}\epsilon\omega(E_x, \phi_x)_{T_d} + \frac{1}{\mu}\left[\left(H_z, \frac{\partial \phi_x}{\partial y}\right)_{T_d} - \langle \hat{H}_z \hat{n}_y, \phi_x\rangle_{\partial T_d}\right] = (J_x, \phi_x)_{T_d} \\ \mathrm{i}\epsilon\omega(E_y, \phi_y)_{T_d} - \frac{1}{\mu}\left[\left(H_z, \frac{\partial \phi_y}{\partial x}\right)_{T_d} - \langle \hat{H}_z \hat{n}_x, \phi_y\rangle_{\partial T_d}\right] = (J_y, \phi_y)_{T_d} \\ \mathrm{i}\omega(H_z, \phi_z)_{T_d} + \left(E_x, \frac{\partial \phi_z}{\partial y}\right)_{T_d} - \left(E_y, \frac{\partial \phi_z}{\partial x}\right)_{T_d} + \langle \hat{E}_y \hat{n}_x - \hat{E}_x \hat{n}_y, \phi_z\rangle_{\partial T_d} = 0 \end{cases} \tag{3.2}$$

holds for any $(\phi_x, \phi_y, \phi_z) \in (X^{\mathcal{N}})^3$ and any $d = 1, \ldots, D$. Here, $(\hat{n}_x, \hat{n}_y)$ is the unit outward normal of the element T_d. The numerical flux $\hat{U}$ (U being E_x, E_y or H_z) is a function of U^-, the limit of U from inside of the element, and U^+, the limit of U from outside of the element. They are defined by

$$\begin{cases} \hat{E}_x = \frac{E_x^+ + E_x^-}{2}, \quad \hat{E}_y = \frac{E_y^+ + E_y^-}{2} & \text{on interior edges,} \\ \hat{E}_y \hat{n}_x - \hat{E}_x \hat{n}_y = 0 & \text{on boundary edges,} \end{cases}$$

$$\hat{H}_z = \begin{cases} \frac{H_z^+ + H_z^-}{2} & \text{on interior edges,} \\ H_z^- & \text{on boundary edges.} \end{cases}$$

Hence, (3.2) can be rewritten as

$$\begin{cases} -\epsilon\omega^2(E_x, \phi_x)_{\Omega^{\mathcal{N}}} - \frac{1}{\mu}\left(D_y^N D_y^D E_x, \phi_x\right)_{\Omega^{\mathcal{N}}} + \frac{1}{\mu}\left(D_y^N D_x^D E_y, \phi_x\right)_{\Omega^{\mathcal{N}}} = \mathrm{i}\omega(J_x, \phi_x)_{\Omega^{\mathcal{N}}} \\ -\epsilon\omega^2(E_y, \phi_y)_{\Omega^{\mathcal{N}}} + \frac{1}{\mu}\left(D_x^N D_y^D E_x, \phi_y\right)_{\Omega^{\mathcal{N}}} - \frac{1}{\mu}\left(D_x^N D_x^D E_y, \phi_y\right)_{\Omega^{\mathcal{N}}} = \mathrm{i}\omega(J_y, \phi_y)_{\Omega^{\mathcal{N}}} \end{cases} \tag{3.3}$$

where the matrices D_x^D, D_x^N are defined by

$$\begin{cases} (g, D_x^D f)_{\Omega^{\mathcal{N}}} = \sum_{d=1}^{D}\left[\left(g, \frac{\partial f}{\partial x}\right)_{T_d} + \left\langle g, \left(\hat{f} - f^-\right)\hat{n}_x\right\rangle_{\partial T_d}\right] \\ \qquad\qquad \text{with} \quad \hat{f} = \begin{cases} \frac{f^- + f^+}{2} & \text{on interior edges} \\ 0 & \text{on boundary edges} \end{cases} \\ (g, D_x^N f)_{\Omega^{\mathcal{N}}} = \sum_{d=1}^{D}\left[\left(g, \frac{\partial f}{\partial x}\right)_{T_d} + \left\langle g, \left(\hat{f} - f^-\right)\hat{n}_x\right\rangle_{\partial T_d}\right] \\ \qquad\qquad \text{with} \quad \hat{f} = \begin{cases} \frac{f^- + f^+}{2} & \text{on interior edges} \\ f^- & \text{on boundary edges} \end{cases} \end{cases}$$

and similarly for D_y^D, D_y^N.

Hence, our bilinear form $a^{\mathcal{N}}(w, v; \nu)$ corresponds to the following matrix:

$$-\epsilon\omega^2 \begin{pmatrix} M & 0 \\ 0 & M \end{pmatrix} + \frac{1}{\mu}\begin{pmatrix} -MD_y^N D_y^D & MD_y^N D_x^D \\ MD_x^N D_y^D & -MD_x^N D_x^D \end{pmatrix}$$

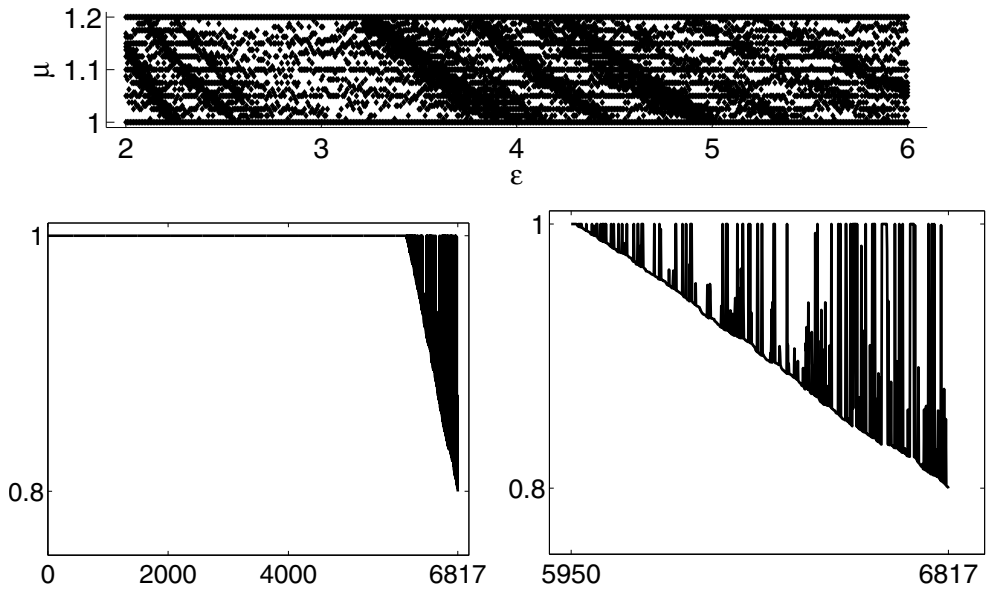

FIGURE 2. Two-dimensional case: The points selected by the *original* SCM and plot of $\frac{\alpha_{UB}-\alpha_{LB}}{\alpha_{UB}}$ in the greedy algorithm.

where the parameter vector $\nu = (\epsilon, \omega, \mu)$ and the matrix M is defined by

$$\vec{g}^T M \vec{f} = (g, f)_{\Omega^{\mathcal{N}}},$$

where $\vec{f}$ is the column vector containing the degrees of freedom of f.

The associated inner product is defined to be the $H(\text{curl})$ norm.

3.2. **Results with two parameters**

We show numerical results for two parameters, $\epsilon_2 \in [2, 6]$, $\mu_2 \in [1.0, 1.2]$. We set $\epsilon_1 = 1$, $\mu_1 = 1$, $\omega = \frac{5\,\pi}{2}$, $M_\alpha = 20$, $M_+ = 6$, $C_1 = \{(2.0, 1.0)\}$, $\epsilon_\alpha = 0.8$ and Ξ is a uniform Cartesian grid of 513×33. This is a pure resonance case in which the inf-sup number goes to zero along the resonance lines.

We first run the original SCM and obtain 6817 points in the parameter space to compute the bounds. The points are plotted in Figure 2. Also plotted here is $\max_{\nu\in\Xi} \frac{\alpha_{UB}(\nu,C_K)-\alpha_{LB}(\nu,C_K)}{\alpha_{UB}(\nu,C_K)}$ for $K = 1, \ldots, 6817$. This quantity is oscillating although it gets below ϵ_α eventually. It may go back to one as shown by the third plot in Figure 2, which means $\alpha_{LB}(\nu_0, C_{K_0}) = 0$ for certain ν_0, K_0 and $\alpha_{LB}(\nu_0, C_K) > 0$ for some $K < K_0$. This phenomenon is a consequence of the looser constraint in (2.2). This motivated the modification in the new definition (2.6).

Next, we run the new SCM with exactly the same settings and obtain 4855 points, plotted in Figure 3. In addition to the fact that the final set of selected points is much smaller, the quantity

$$\max_{\nu\in\Xi} \frac{\alpha_{UB}(\nu, C_K) - \alpha_{LB}(\nu, C_K)}{\alpha_{UB}(\nu, C_K)}$$

decreases monotonically until smaller than ϵ_α, as shown in Figure 3.

As shown by both Figures 2 and 3, the method selects points along several lines which are exactly where the resonance occurs. We plot in Figures 4 and 5 the lower and upper bound computed by the new SCM on the set C_{4855}. We observe that the lower bound is very close to the upper bound and the 12 resonance lines

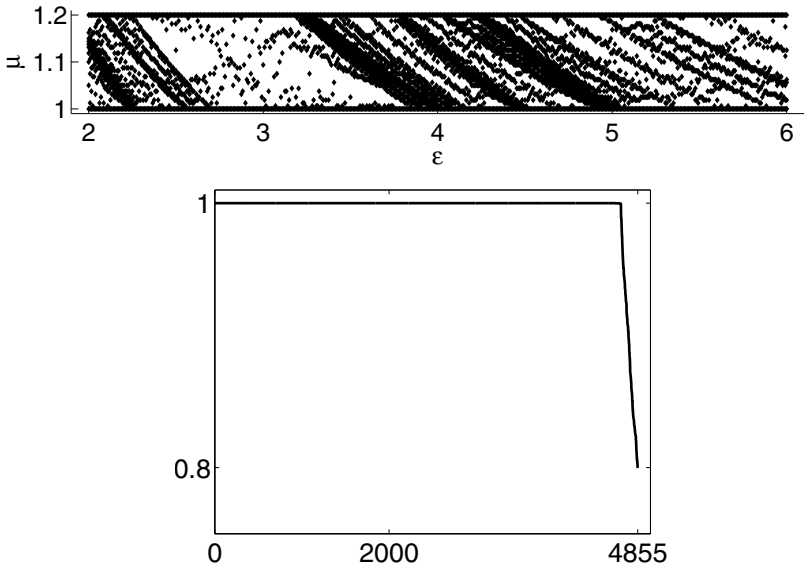

FIGURE 3. Two-dimensional case: The points selected by the *new* SCM and plot of $\frac{\alpha_{UB}-\alpha_{LB}}{\alpha_{UB}}$ in the greedy algorithm.

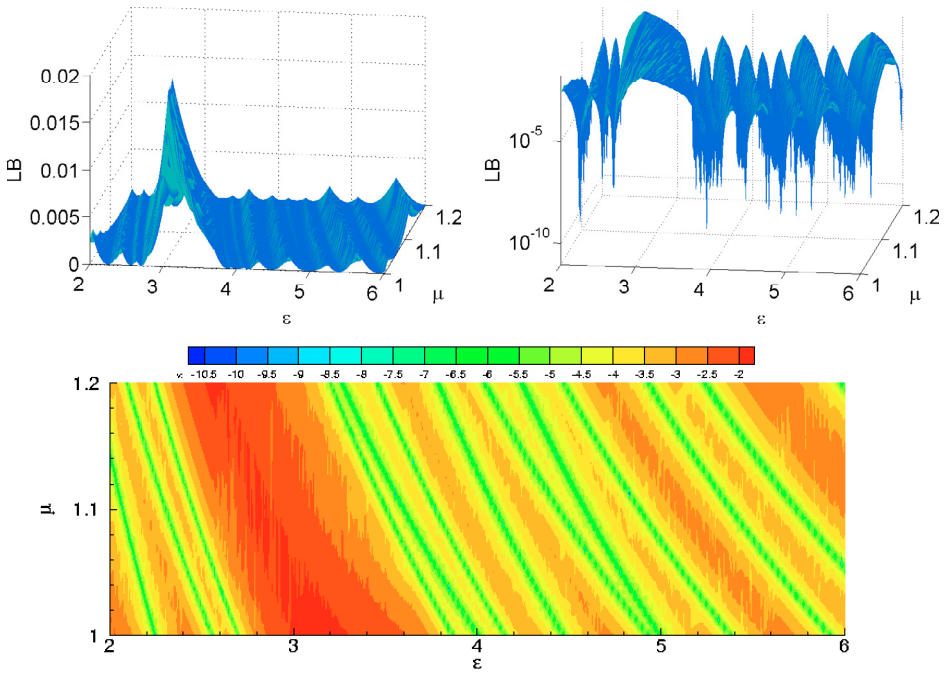

FIGURE 4. Lower bound of the square of the inf-sup constant computed by the *new* SCM in two-dimensional case: the first is in linear scale, the second in logarithmic scale and the third being the contour plot of the logarithm.

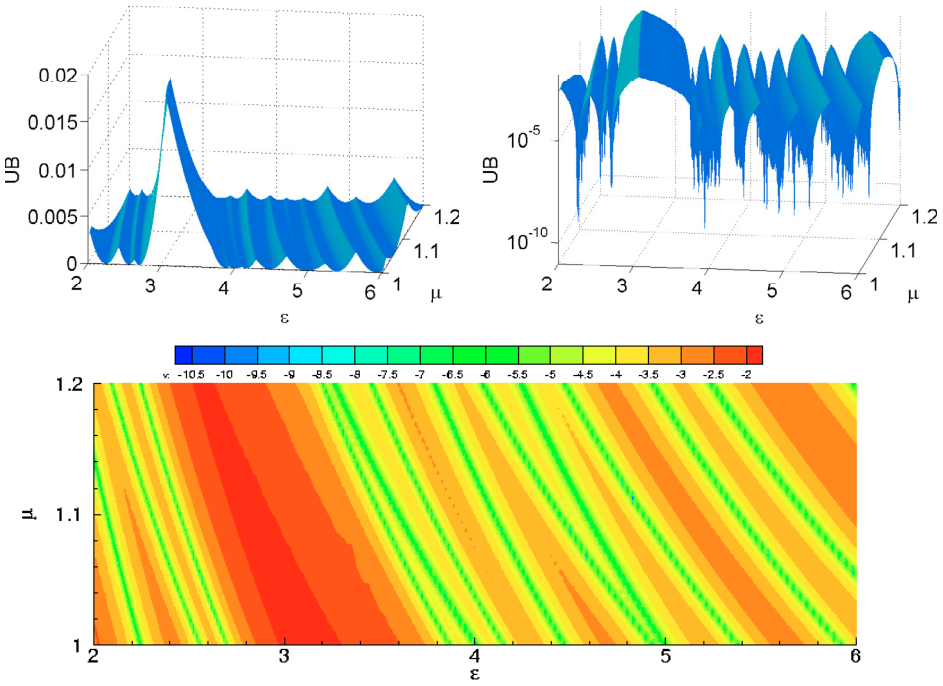

FIGURE 5. Upper bound of the square of the inf-sup constant computed by the *new* SCM in two-dimensional case: the first is in linear scale, the second in logarithmic scale and the third being the contour plot of the logarithm.

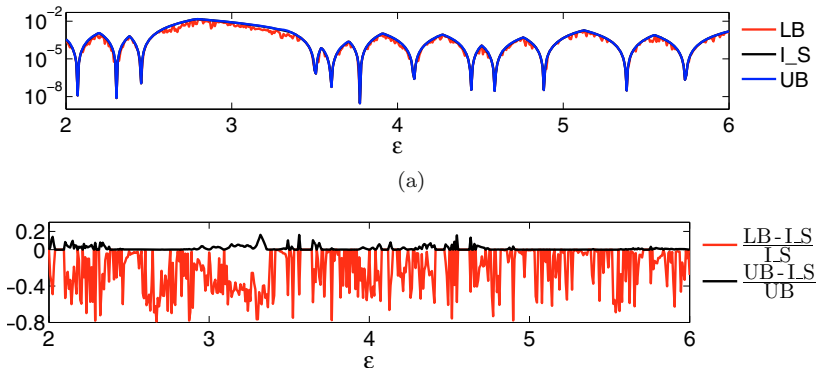

FIGURE 6. The lower bound (LB), square of Inf-Sup (I-S) constant and upper bound (UB) on the line with $\mu_2 = 1.1$ in the two-dimensional case: (a) is for the three quantities and (b) is for the two ratios.

in our parameter domain are clearly identified. Moreover, the lines agree with the theory that provides an analytic expression for the resonance lines satisfying $\epsilon.\mu =$ constant.

To see the quality of our lower bounds and upper bounds to approximate the true value, *i.e.*, the square of the Inf-Sup constant, we compute the exact Inf-Sup constants along the line $\mu_2 = 1.1$. The results are plotted in Figure 6 where we observe that the bounds are, in fact, effective and sharp.

FIGURE 7. Three-dimensional case: The points selected by the *new* SCM on the face $\Im\epsilon_2 = 0$.

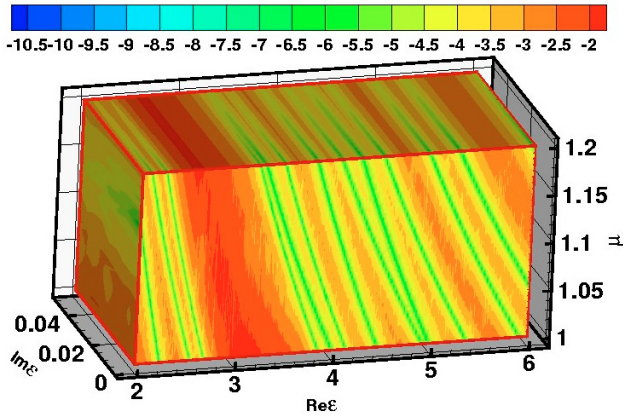

FIGURE 8. Contour plot of the logarithm of lower bound computed by the *new* SCM in three-dimensional case.

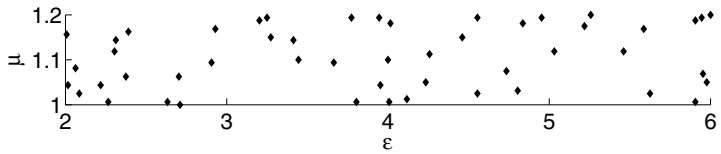

FIGURE 9. The points selected by the RBM to build the bases for the test problem.

3.3. **Results with three parameters**

Here, we show numerical results for three parameters, $\Re\epsilon_2 \in [2, 6]$, $\Im\epsilon_2 \in [0, 0.05]$, $\mu_2 \in [1.0, 1.2]$. We set $\epsilon_1 = 1$, $\mu_1 = 1$, $\omega = \frac{5\pi}{2}$, $M_\alpha = 30$, $M_+ = 9$, $C_1 = \{(2.0, 0.0, 1.0)\}$, $\epsilon_\alpha = 0.8$ and Ξ is a uniform Cartesian grid of $513 \times 9 \times 33$. We run the SCM and obtain 36 363 points in the parameter space. The points selected on the face $\Im\epsilon_2 = 0$ are plotted in Figure 7. Not surprisingly, the set is very similar to that in the case of two parameters. Plotted in Figure 8 is the contour plot of the lower bound. We point out, again, that the contour on the face $\Im\epsilon_2 = 0$ is almost the same as that for the two-parameter case.

3.4. **Application to error estimate for the reduced basis method**

Having obtained the lower bound of the inf-sup number, we can apply it to the *a posteriori* error estimate (1.2) which is essential to build the reduced basis space. One algorithm for the construction of the reduced basis spaces are outlined as follows, see [2,6,12,14,15,17] for details:

- Choose, arbitrarily, $\nu_1 \in \Xi$ as the first parameter.
- Compute $u^{\mathcal{N}}(\nu_1)$.
- Initialize the reduced basis space $W^1 = \text{span}\{u^{\mathcal{N}}(\nu_1)\}$.

- For $j = 2 \ldots N$:
  - Choose the next parameter as $\nu_j = \text{argmax}_{\nu \in \Xi} \frac{\|r(\cdot,\nu)\|_{(X^{\mathcal{N}})'}}{\beta_{LB}(\nu)}$.
  - Compute $u^{\mathcal{N}}(\nu_j)$.
  - Update the reduced basis space as $W^j = \text{span}\{u^{\mathcal{N}}(\nu_i),\ i \in \{1, \ldots, j\}\}$.

Clearly, the final sample set is $\{\nu_1, \ldots, \nu_N\}$ and the final reduced basis space is $W^N = \text{span}\{u^{\mathcal{N}}(\nu_i),\ i \in \{1, \ldots, N\}\}$. Since W^N is hierarchical, we also obtain the reduced basis spaces of any dimension lower than N. In this paper, we take $N = 50$ and build W^{50} for the two-parameter case as in Section 3.2. See Figure 9 for the final sets $\{\nu_1, \ldots, \nu_{50}\}$.

Then, we use this space to compute the reduced basis solution for any parameter. See Figure 10 for sample solutions at $(\epsilon_1, \mu_1) = (2, 1)$. Here, we show the truth approximation and the RB solutions with the dimension of the RB spaces being 10, 20, and 30. We can see that, as we increase the dimension of the RB space, the RB solution approximates the truth approximation better and better. Actually, the $H(\text{curl})$ norm of the error between the RB solution and the truth approximation is decreasing exponentially. We also list, in the last column, the relative CPU time to obtain these approximations. It is easy to conclude that the on-line computation time for the RB solution is negligible compared to that of the truth approximation.

Next, we test our error estimate on a set of 1300 points in the parameter domain, see Figure 11 for the set, $\Xi_{\text{train}} \subset \Xi \backslash \{\nu_1, \ldots, \nu_N\}$. We first pick three points in Ξ_{train} which have the largest, median and smallest lower bounds for the inf-sup number. The truth approximations are shown in Figure 12 together with the error and error estimate of the RB solution computed using 30 reduced bases. We see that, even if the truth approximations are very different with varying parameter configurations, the reduced basis solution converges to the truth approximation nicely and it is indicated by the error estimate effectively.

We then compute, for any $\nu \in \Xi_{\text{train}}$, the truth approximation and the reduced basis solutions for $N = 10, \ldots, 30$ and evaluate the energy and $H(\text{curl})$ norms of the error $u^{\mathcal{N}}(\nu) - u^N(\nu)$ and the error estimate $\frac{\|r(\cdot,\nu)\|_{(X^{\mathcal{N}})'}}{\beta_{LB}(\nu)}$. In Figures 13a–13c, we plot the maximum, median, and minimum of these values over Ξ_{train} and observe that all basically decrease exponentially with respect to N.

Note that the truth approximations have very strong singularity. Hence, when 30 reduced bases are used, the RB solution has error around 10^{-5} and error indicator around 10^{-2} in the worst case. This is still meaningful since the error of the truth approximations (evaluated between the truth solution and the solution obtained on the same mesh with piecewise polynomials of degree ≤ 7) is at about this level. Another reason for the behavior of the error estimate in the worst case is that the lower bound of the inf-sup number, $\beta^{\mathcal{N}}(\nu)$, is rather small. In fact, all the worst cases for $N > 12$ in Figure 13c take place on the ν's that have lower bound smaller than the median lower bound in Ξ_{train}. It is also worth mentioning that the quality of the error estimate could be improved by building the estimate on the energy norm rather than on the $H(\text{curl})$ norm.

Finally, we have sorted Ξ_{train} according to the corresponding lower bound and let Ξ^k_{train} be the set of the first k points in Ξ_{train} for $k = 1, \ldots, 1300$. Figure 13d represents the the maximum effectivity indices over Ξ^k_{train} *versus* k for reduced basis spaces of dimensions 10, 15, 20, 25. We see that the error estimate is sharper as the parameter stays further away from the resonances. It is interesting however to note also that the effectivity indices are rather independent of the size of the reduced basis that is used for the computation. That is, the effectivity indices remain of the same magnitude when the errors become many magnitudes smaller as we increase the dimension of the reduced basis space. Hence, the method provides a quite reliable *a posteriori* estimator for the actual error.

4. Concluding remarks

We have improved the currently available best method we are aware of for the construction of lower bounds for the coercivity and inf-sup stability constants. The new method is more efficient, more robust and has a nice property, namely, the computed lower bound is monotonically increasing with respect to the size of the nested sets its construction is based on. We have applied this method to construct the lower bound of the inf-sup constant of a challenging electromagnetic cavity problem. The projected enhancements are confirmed

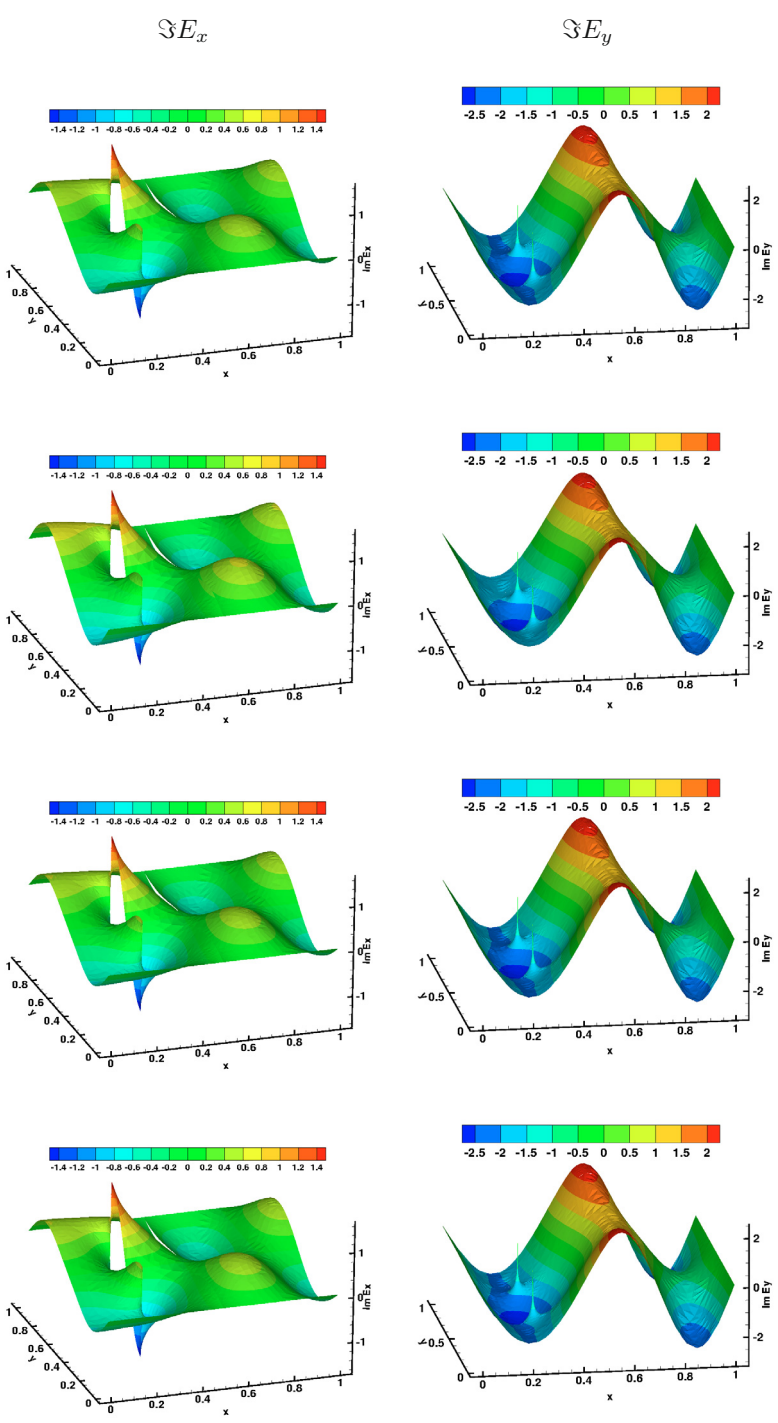

FIGURE 10. Sample solutions at $(\epsilon, \mu) = (2.0, 1.0)$: the truth (first row) and reduced basis approximations with 10 (second), 20 (third), and 30 (last) bases. "Error" denotes the $H(\text{curl})$ difference from the truth approximation; "Time" means the relative on-line computation time.

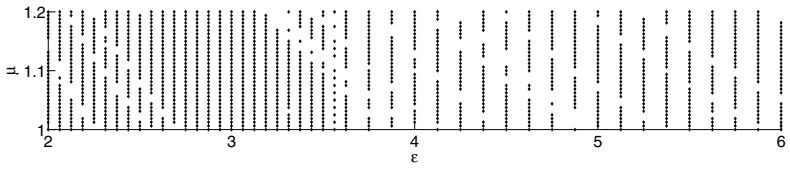

FIGURE 11. Ξ_{train} contains 1300 points.

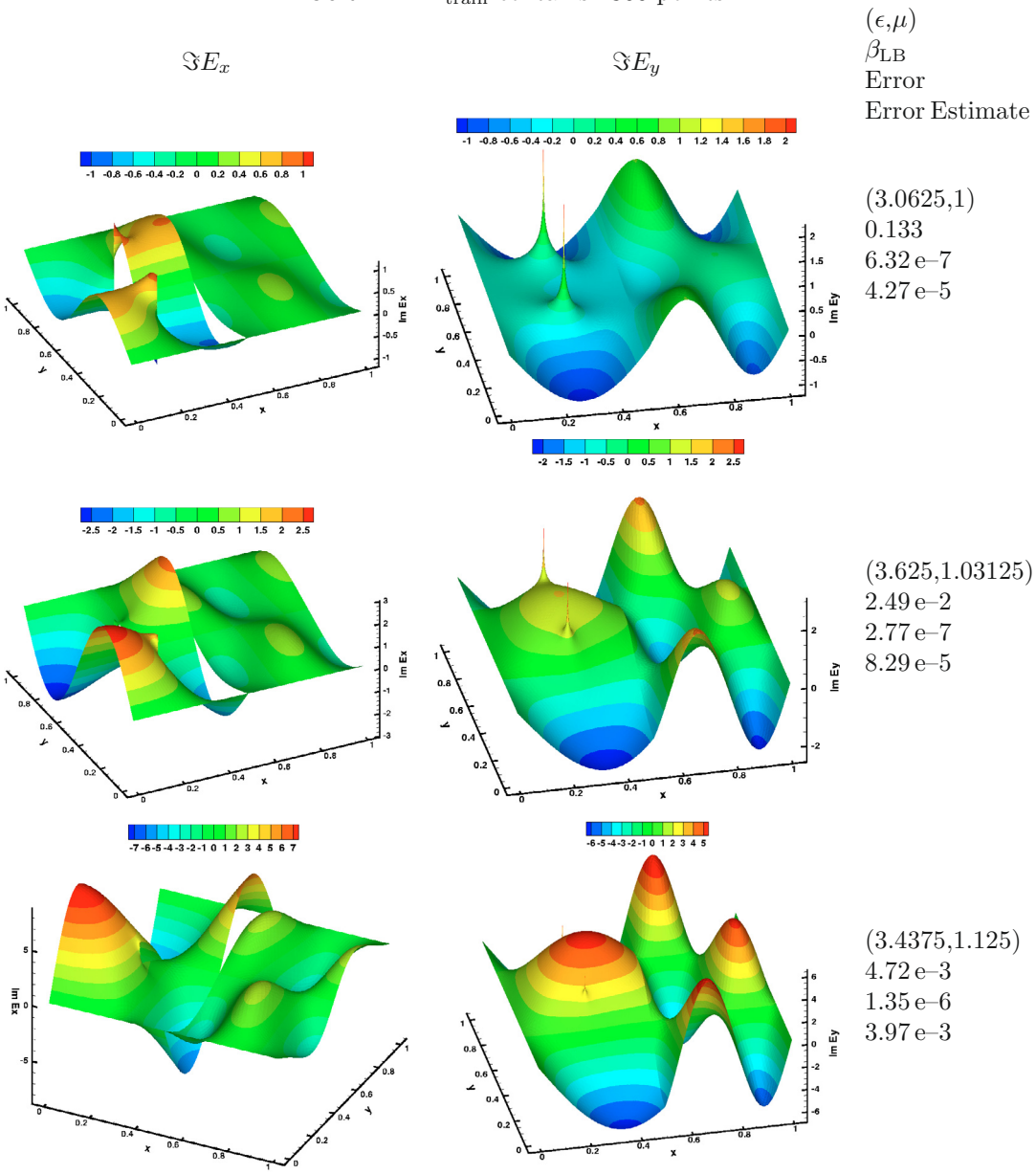

FIGURE 12. Sample truth solutions with different parameter configurations. "Error" denotes the $H(\text{curl})$ norm of the difference between the truth approximation (shown) and the reduced basis solution with 30 basis (not shown).

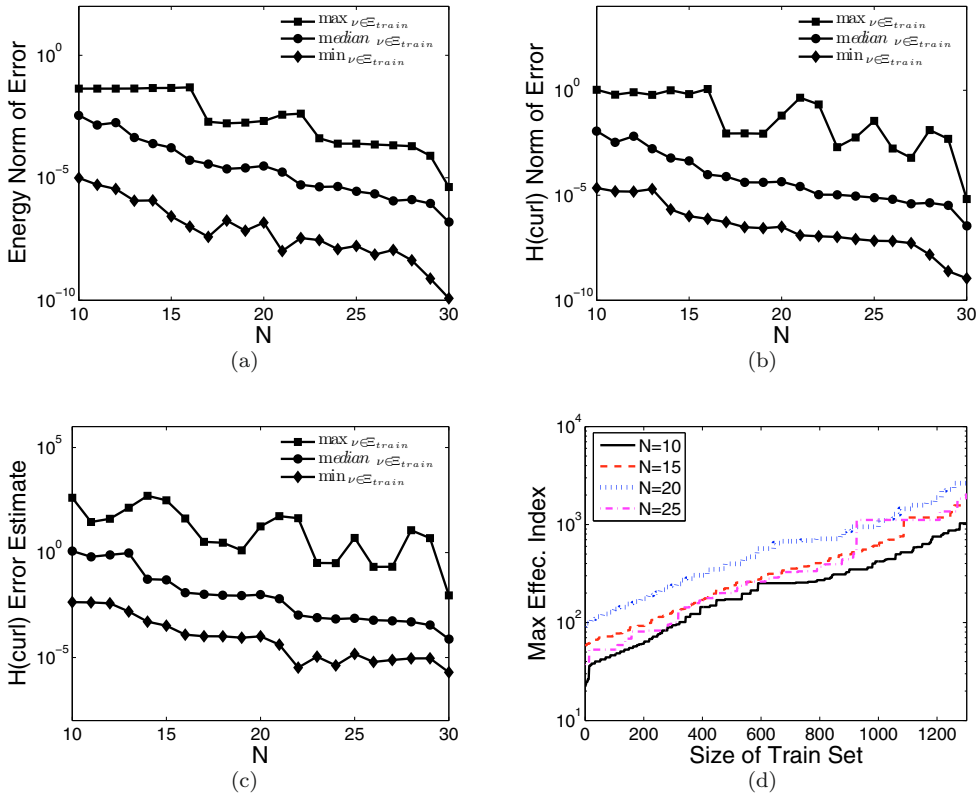

FIGURE 13. (a) The dimensions of the reduced basis space *versus* the energy norm of the errors of the solution. (b) The dimensions of the reduced basis space *versus* the $H(\mathrm{curl})$ norm of the errors of the solution. (c) The dimensions of the reduced basis space *versus* the $H(\mathrm{curl})$ error estimate. (d) The size of the train set *versus* the maximum effectivity index of the error estimates.

by the numerical results; the method captures the resonance lines very accurately. Moreover, we have applied the constructed lower bounds to the error estimate for the reduced basis approximation. The resulting method is very efficient. Exponential convergence of the reduced basis approximation to the truth finite element approximation are confirmed.

Future works include efficient strategies to deal with problems with high-dimensional parameter spaces. In such cases, using the greedy algorithm based on uniform Cartesian grids to determine the set C_K and the reduced basis space W_N becomes very expensive. One possible direction is to combine these greedy type algorithms with some adaptive sampling approach similar to the one used in [3].

Acknowledgements. Research supported by AFOSR Grant FA9550-07-1-0425. The authors thank the anonymous referee for calling their attention to reference [3].

REFERENCES

[1] M. Barrault, N.C. Nguyen, Y. Maday and A.T. Patera. An empirical interpolation method: Application to efficient reduced-basis discretization of partial differential equations. *C. R. Acad. Sci. Paris Ser. I Math.* **339** (2004) 667–672.

[2] A. Barret and G. Reddien, On the reduced basis method. *Z. Angew. Math. Mech.* **75** (1995) 543–549.

[3] T. Bui-Thanh, K. Willcox and O. Ghattas, Model reduction for large-scale systems with high-dimensional parametric input space. *SIAM J. Sci. Comput.* **30** (2008) 3270–3288.
[4] Y. Chen, J.S. Hesthaven, Y. Maday and J. Rodríguez, A monotonic evaluation of lower bounds for Inf-Sup stability constants in the frame of reduced basis approximations. *C. R. Acad. Sci. Paris Ser. I Math.* **346** (2008) 1295–1300.
[5] M.A. Grepl, Y. Maday, N.C. Nguyen and A.T. Patera. Efficient reduced-basis treatment of nonaffine and nonlinear partial differential equations. *ESAIM: M2AN* **41** (2007) 575–605.
[6] M.D. Gunzburger, *Finite element methods for viscous incompressible flows.* Academic Press (1989).
[7] J.S. Hesthaven and T. Warburton, *Nodal Discontinuous Galerkin Methods: Algorithms, Analysis, and Applications*, *Springer Texts in Applied Mathematics* **54**. Springer Verlag, New York (2008).
[8] D.B.P. Huynh, G. Rozza, S. Sen and A.T. Patera, A successive constraint linear optimization method for lower bounds of parametric coercivity and inf-sup stability constants. *C. R. Acad. Sci. Paris Ser. I Math.* **345** (2007) 473–478.
[9] L. Machiels, Y. Maday, I.B. Oliveira, A.T. Patera and D. Rovas, Output bounds for reduced-basis approximations of symmetric positive definite eigenvalue problems. *C. R. Acad. Sci. Paris Ser. I Math.* **331** (2000) 153–158.
[10] Y Maday, *Reduced Basis Method for the Rapid and Reliable Solution of Partial Differential Equations*, in *Proceeding ICM Madrid* (2006).
[11] Y. Maday, A.T. Patera and D.V. Rovas, A blackbox reduced-basis output bound method for noncoercive linear problems, in *Nonlinear Partial Differential Equations and Their Applications*, D. Cioranescu and J.L. Lions Eds., *Collège de France Seminar* **XIV**, Elsevier Science B.V. (2002) 533–569.
[12] D.A. Nagy, Modal representation of geometrically nonlinear behaviour by the finite element method. *Comput. Struct.* **10** (1979) 683–688.
[13] N.C. Nguyen, K. Veroy and A.T. Patera. Certified real-time solution of parametrized partial differential equations, in *Handbook of Materials Modeling*, S. Yip Ed., Springer (2005) 1523–1558.
[14] A.K. Noor and J.M. Peters, Reduced basis technique for nonlinear analysis of structures. *AIAA Journal* **18** (1980) 455–462.
[15] J.S. Peterson, The reduced basis method for incompressible viscous flow calculations. *SIAM J. Sci. Stat. Comput.* **10** (1989) 777–786.
[16] C. Prud'homme, D. Rovas, K. Veroy, Y. Maday, A.T. Patera and G. Turinici, Reliable realtime solution of parametrized partial differential equations: Reduced-basis output bound methods. *J. Fluids Engineering* **124** (2002) 70–80.
[17] G. Rozza, D.B.P. Huynh and A.T. Patera, Reduced basis approximation and a posteriori error estimation for affinely parametrized elliptic coercive partial differential equations: Application to transport and continuum mechanics. *Arch. Comput. Methods Eng.* **15** (2008) 229–275.
[18] S. Sen, K. Veroy, D.B.P. Huynh, S. Deparis, N.C. Nguyen and A.T. Patera, "Natural norm" a posteriori error estimators for reduced basis approximations. *J. Comput. Phys.* **217** (2006) 37–62.